Published in final edited form as:

Breast Cancer Res Treat. 2014 December ; 148(3): 489–499. doi:10.1007/s10549-014-3180-7.

A Novel Vaccinia Virus with Dual Oncolytic and Anti-angiogenic Therapeutic Effects against Triple-Negative Breast Cancer

Sepideh Gholami, MD[1,*], **Andrew Marano, BA**[1,*], **Nanhai G. Chen, PhD**[2,3], **Richard J. Aguilar**[2], **Alexa Frentzen, PhD**[2], **Chun-Hao Chen, MD**[1], **Emil Lou, MD, PhD**[4], **Sho Fujisawa, PhD**[5], **Clarisse Eveno, MD, PhD**[1], **Laurence Belin, MD, MPH**[1], **Pat Zanzonico, PhD**[6], **Aladar Szalay, PhD**[2,3,7], and **Yuman Fong, MD**[1,8]

[1]Department of Surgery, Memorial Sloan-Kettering Cancer Center, New York, NY, United States

[2]Genelux Corporation, San Diego Science Center, San Diego, CA 92109, United States

[3]Department of Radiation Medicine and Applied Sciences, Rebecca & John Moores Comprehensive Cancer Center, University of California, San Diego, CA 92093, United States

[4]University of Minnesota, Department of Medicine, Division of Hematology, Oncology, and Transplantation, Minneapolis, MN, United States

[5]Molecular Cytology Core Facility, Memorial Sloan-Kettering Cancer Center, New York, NY, United States

[6]Departments of Medical Physics and Radiology, Memorial Sloan-Kettering Cancer Center, New York, NY 10065, United States

[7]Rudolf Virchow Center for Experimental Biomedicine, Department of Biochemistry and Institute for Molecular Infection Biology, University of Würzburg, Am Hubland, D-97074 Würzburg, Germany

[8]Department of Surgery, City of Hope Medical Center, Duarte, CA, United States

Abstract

Purpose—Vascular endothelial growth factor (VEGF) expression is higher in triple-negative breast cancers (TNBC) compared to other subtypes and is reported to predict incidence of distant metastases and shorter overall survival. We investigated the therapeutic impact of a vaccinia virus (VACV) GLV-1h164 (derived from its parent virus GLV-1h100), encoding a single-chain antibody (scAb) against VEGF (GLAF-2) in an orthotopic TNBC murine model.

Methods—GLV-1h164 was tested against multiple TNBC cell lines. Viral infectivity, cytotoxicity, and replication were determined. Mammary fat pad tumors were generated in

Corresponding author: Yuman Fong, MD, Chairman, Department of Surgery, City of Hope Medical Center, 1500 East Duarte Road, Duarte, CA 91010, Phone: (626) 218-9172, Fax: (626) 471-9212, E-mail: yfong@coh.org.

*These authors contributed equally to this work

CONFLICT OF INTEREST

Nanhai Chen, Richard J. Aguilar, Alexa Frentzen, and Aladar Szalay are employees of Genelux corporation. None of the other authors of this manuscript have any conflict of interest associated with this work.

athymic nude mice using MDA-MB-231 cells. Xenografts were treated with GLV-1h164, GLV-1h100, or PBS and followed for tumor growth.

Results—Viral infectivity was time- and concentration-dependent. GLV-1h164 killed TNBC cell lines in a dose-dependent fashion with greater than 90% cytotoxicity within 4 days at a multiplicity of infection of 5.0. *In vitro*, cytotoxicity of GLV-1h164 was identical to GLV-1h100. GLV-1h164 replicated efficiently in all cell lines with an over 400-fold increase in copy numbers from the initial viral dose within 4 days. *In vivo*, mean tumor volumes after 2 weeks of treatment were 73, 191, and 422mm^3 (GLV-1h164, GLV-1h100, and PBS, respectively) ($p<0.05$). Both *in vivo* Doppler ultrasonography and immuno-staining showed decreased neo-angiogenesis in GLV-1h164-treated tumors compared to both GLV-1h100 and PBS controls ($p<0.05$).

Conclusion—This is the first study to demonstrate efficient combination of oncolytic and anti-angiogenic activity of a novel vaccinia virus on TNBC xenografts. Our results suggest that GLV-1h164 is a promising therapeutic agent that warrants testing for patients with TNBC.

Keywords

Vaccinia virus; oncolytic viral therapy; GLV-1h164; anti-angiogenesis; triple-negative breast cancer

INTRODUCTION

Triple-negative breast cancer (TNBC) is a particularly aggressive subtype of breast cancer for which there are currently no effective forms of targeted therapy. The hallmark of TNBCs is their lack of expression of estrogen and progesterone receptors, as well as the lack of over-expression of the human epidermal growth factor 2 (Her2) receptor. This lack of expression precludes use of a number of therapeutic agents commonly used to treat other hormone and EGFR-expressing forms of breast cancer [1]. Additionally, TNBCs are associated with high rates of recurrence and carry a poor prognosis; patients with TNBC have a reduced overall survival [2,3]. This form of the disease is most common in younger African-American and Hispanic women and constitutes approximately 15% of all breast cancers [3,1]. TNBCs represent a highly proliferative form of malignancy and depend on stimulation of new blood vessel growth. Studies have shown that vascular endothelial growth factor (VEGF) content of human TNBC tumors was 3 times higher compared with other subtypes [4]. VEGF is a mediator of angiogenesis and has thus become a target for TNBC therapy. Previous studies have shown the importance of angiogenesis to tumor growth and the effectiveness of antiangiogenic agents. Bevacizumab, an agent that targets the VEGF pathway, has been shown to significantly improve progression-free survival and objective response rate in human trials in breast cancer when administered in combination with other cancer therapy drugs [5]. Other researchers have demonstrated that ellagic acid, another antiangiogenic agent, significantly inhibits cancer growth in TNBCs specifically [6]. Novel antiangiogenic agents have notable biologic activity in the treatment of TNBC and merit further investigation.

In our laboratory, we have previously shown that vaccinia virus can infect, replicate in, and kill cancer cells, including anaplastic thyroid [7], pancreatic [8], gliomas [9], and breast

[10], specifically including TNBC [11]. GLV-1h164 is an oncolytic vaccinia virus strain that contains the single-chain antibody sequence for GLAF-2, an antibody directed against VEGF. Previous research has shown that GLAF is highly expressed in pancreatic cells infected with anti-VEGF vaccinia constructs and that it possesses significant inhibitory effects on the development of blood vessels [12]. Moreover, this viral construct has demonstrated significantly improved tumor therapy in xenografts compared to the parent virus. The success of both antiangiogenic agents and the oncolytic vaccinia virus in treating cancer has led us to the objective of this study: to investigate the therapeutic efficacy of this novel vaccinia strain in TNBC cell lines and our established TNBC mammary fat pad xenograft model.

MATERIALS AND METHODS

Cell Lines

Human TNBC cell lines MDA-MB-468, HCC-1143, HCC-1806 and African green monkey kidney fibroblasts (CV-1) were obtained from American Type Culture Collection (American Type Culture Collection, Manassas, VA USA). Human MDA-MB-231 breast carcinoma cells stably expressing mCherry fluorescent protein (kindly provided by Dr. Koblinski from Northwestern University) were maintained in Dulbecco's modified Eagle's medium (DMEM)/F12 supplemented with 5% FBS, 100 IU/ml penicillin/streptomycin, 1 mM sodium pyruvate, 2× nonessential amino acids and 1μg/ml blasticidin (Sigma-Aldrich, St. Louis, MO USA). MDA-MB-468 cells were maintained in DMEM supplemented with 5% FBS, 100 IU/ml penicillin/streptomycin, 1 mM sodium pyruvate, 2× nonessential amino acids. HCC1143 and 1806 cell lines were maintained in RPMI supplemented with 10 mM Hepes, 2 mM L-glutamine, 1mM sodium pyruvate, 1.5g/L sodium bicarbonate, and 4.5g/L glucose. CV-1 cells were maintained in Minimum Essential Medium (MEM). Unless otherwise specified, all media were supplemented with 10% FCS and penicillin (100,000 U/L) and streptomycin (100 mg/L) and cells were grown in a 5% CO_2 humidified incubator at 37°C.

Generation of GLV-1h100 and GLV-1h164

The plasmid 0608997-pGA4 [12] was used as a template to amplify GLAF-2 scAb from the GLAF-1 scAb sequence with the primers G6-for-b (5′-GTCGACCCACCATGGAGAC-3′) and G6-rev-b (5′TTAATTAATTATCGCTTAATCTCAACCTTGGTCCC-3′) thereby deleting the DDDDK tag. The sequence GLAF-2 was subcloned into pCRII-TOPO (Invitrogen). The GLAF-2 fragment was cloned into the framework plasmid via the SalI and PacI sites, yielding the plasmid pHA-PSL-GLAF-2. GLV-1h164 was generated from GLV-1h100 using pHA-PSL-GLAF-2. All recombinant viruses were constructed using the method described previously [13]. The genotype of each recombinant virus was confirmed by PCR and sequencing. Viral constructs are illustrated in Figure 1a.

Green Fluorescent Protein Expression

Cells were plated at 1.5×10^4 cells/well in 96-well plates and incubated overnight. Cells were infected with GLV-1h164 at multiplicities of infection (MOIs) of 1, 5, and 10. At 1, 2, and 3

days post-infection, pictures were taken with a inverted fluorescence microscope (Nikon Eclipse TE300; Nikon, Tokyo, Japan).

Cytotoxicity Assay

Cells were plated at 3×10^4 cells/well in 24-well plates and incubated overnight. Cells were then infected with either GLV-1h164 or GLV-1h100 at MOIs of 0.1, 1, and 5, and media was concurrently replaced in the controls. Cells were lysed daily for 5 days after treatment with 1.35% Triton-X solution to release lactate dehydrogenase (LDH). LDH was measured with a Cytotox 96 nonradioactive cytotoxicity assay (Promega, Madison, WI) on a spectrophotometer (EL321e, Bio-Tek Instruments, Winooski, VT) at 490 nm. The result is expressed as the percentage of surviving cells, calculated by comparison of LDH release in infected cells versus negative controls.

Viral Replication Assay

Viral replication in TNBCs was quantified using a standard plaque assay. TNBCs were plated at 3×10^5 in 6-well flat-bottom assay plates in 2 mL of media and incubated at 37°C. Cells were infected with either virus (GLV-1h164 or GLV-1h100) at MOIs 1 and 5, and supernatants were harvested daily for a total of 4 days. Serial dilutions of each sample were used to infect CV-1 cells on confluent 12-well plates, and viral titers were determined by counting viral plaques after 72 hours.

GLAF-2 Expression

MDA-MB-468 cells were infected with either virus strain at an MOI of 1. At 24 and 48 hours post infection, cell lysates and culture supernatants were collected. Proteins were denatured and analyzed with SDS-PAGE. 20 μg protein samples were loaded on 4–20% Tris-HCl buffered gels using the Bio-rad system (Bio-Rad Laboratories, San Francisco, CA). After electrophoresis, proteins were transferred to a PVDF membrane and blocked in 5% milk in Tris-buffered saline with Tween-20 (TBST). Membranes were incubated with a (rabbit) antibody against GLAF-2 (Genelux, San Diego, CA) at a concentration of (1: 5000) and incubated overnight at 4°C. After washing with TBS-T, horseradish peroxidase-conjugated goat anti-rabbit IgG (Santa Cruz, Santa Cruz, CA) was applied for 1hour, followed by enhanced chemiluminescence Western blotting detection reagents (Amersham, Arlington Heights, IL).

In Vivo Tumor Therapy

Thirty-three female athymic nude mice (Hsd: athymic Nude-*Foxn1*^{nu}) aged 6–8 weeks were injected with 5×10^6 MDA-MB-231 mCherry cells suspended in 50% matrigel into the mammary fat pad. Two weeks after tumor implantation, mice were sorted randomly into three groups and injected intratumorally with either PBS, GLV-1h100, or GLV-1h164 (1×10^6). Tumor growth was measured every 3 days over the course of 3 weeks. Tumor volumes were calculated by the equation, $V\ (mm^3) = (4/3)*(\pi)*((a/2)^2*(b/2))$ where ‘a’ is the smallest diameter and ‘b’ the largest diameter. 3 weeks after treatment, mice were sacrificed and tumors and organs (lung, kidney, spleen, ovaries, and heart) were harvested

and frozen for further immunofluorescence staining, histopathology review, and viral plaque assay.

In vivo viral plaque assay

At the end of treatment in our orthotopic model, 3 mice each from the treatment and control group were euthanized and tumors and organs (lung, heart, ovaries, kidney, and spleen) were excised, weighed, inspected, and homogenized in 0.5 ml of PBS containing proteinase inhibitors using MagNA Lyser (Roche Diagnostics, Indianapolis, IN) at a speed of 6500 rpm for 3 min. After three cycles of freeze and thaw, the supernatants were collected by centrifugation at 1200 rpm for 5 min. The viral titers were determined in duplicate by standard plaque assays on confluent 12-well plates of CV-1 cells.

Doppler Ultrasonography

A separate group of animals was treated as mentioned above. After 3 weeks of treatment, animals were imaged by Doppler ultrasound using a dedicated small-animal ultrasound system (Vevo 2100, Visualsonics, Toronto, Canada). To ensure that the tumor size was not a confounding factor, tumors of similar sizes from each treatment group were selected.

Tissue preparation

To prepare tissue sections for HE and IF, tissues were fixed with 4% paraformaldehyde in PBS overnight at 4°C, washed in 70% ethanol and processed for paraffin embedding per the standard protocol of the Molecular Cytology Core Facility of MSKCC. Five micron serial sections were cut from paraffin-embedded tumor tissue blocks. Slides were air dried and baked at 60°C for 1 hour. Immunofluorescence and H&E staining were performed to detect the presence of vascular density in treated versus control tumors. H&E slides were reviewed by a breast pathologist at MSKCC.

Immunofluorescence and H&E staining

IF was performed with the primary antibodies, rat polyclonal anti-MECA-32 (DSHB, 3μg/mL) and chicken polyclonal anti-GFP (Abcam, 2μg/mL) by automated Ventana XT machine. Slides were first blocked with blocking solution (10 % Normal Goat Serum in 2 % BSA in PBS) for 10 min. Primary antibody incubation lasted 6 hours at 37°C, followed by 60 minutes of incubation with biotinylated rabbit anti-rat and biotinylated goat-anti chicken secondary antibodies from ABC Vectastain kit (Vector Laboratories; 7.5ug/mL). Detection was performed with DABMap kit (Ventana Medical Systems) and Tyramide Signal Amplification Alexa Fluor 488 (Invitrogen TSA kit). Tissue slides were counterstained with DAPI (Sigma Aldrich, 10ug/ml) for 10 min at room temperature. IF stained slides were digitally scanned with Zeiss Mirax Scan with 20×/0.8NA objective. Images obtained from the scanner were imported to Metamorph (BioVision) where appropriate threshold values for MECA-32 and DAPI were set. Thresholded area of MECA-32 was normalized to the thresholded area of DAPI. Total of 15 images from 3 individual sections per treatment group were analyzed. H&E staining of tissue sections were performed per routine protocols and reviewed by a breast pathologist at MSKCC.

Statistical Analysis

Results are reported as means with standard errors. Significance of the difference between different groups was calculated using Student's t-test. Differences were deemed significant if the p-value was less than 0.05.

RESULTS

Viral infection is time- and dose-dependent *in vitro*

GFP expression was evaluated in four TNBC cell lines at 24, 48, and 72 hours post-infection. Expression was visible in all cell lines and increased with time, as evidenced by the increasing number of green cells and intensity of the green signal as time increases in Figure 1b. Nearly 100% of cells expressed GFP by day 3 post-infection. In addition, GFP expression also increased with increasing dose, as seen by the same trend across increasing MOIs in Figure 1c. With increasing MOI (MOI 10 compared to MOI 1), almost all cells were infected within 48 hours post infection.

Cytotoxicity in human TNBC cell lines is time- and dose-dependent *in vitro*

All cell lines were sensitive to GLV-1h164 and greater cytotoxicity was measured both at later time points and higher MOIs (Fig. 2a). Greater than 90% cell kill was achieved by day 4 at MOI 5 in all TNBC cell lines. Compared to the parent virus, GLV-1h100, there was no significant difference in the cytotoxicity pattern (Fig. 2b).

GLV-1h164 replicates effectively in all TNBC cell lines *in vitro*

4 TNBC cell lines were treated with GLV-1h164 or GLV-1h100 at an MOI of 1 and viral replication was measured each day for 4 days post-infection. All cell lines supported replication of both viral constructs and, by day 4, plaque-forming units (PFUs) increased up to 650-fold from the initial viral dose. Furthermore, there was no significant difference in the replication efficiency between the two vaccinia strains (Fig. 3).

Anti-VEGF scAb protein is expressed in infected MDA-MB-468 cells

Cells were infected with either viral construct at an MOI of 1 and the lysates and culture supernatants were collected at 24- and 48-hour time points. Western blot analysis revealed anti-VEGF antibody GLAF-2 expression in GLV-1h164-infected cells and their supernatants, but not in the negative control or parent virus treatment groups. In addition, culture supernatant samples suggested increased expression at the later time point whereas cell lysate samples showed similar expression at both time points (Fig. 4).

GLV-1h164 causes significant tumor regression in TNBC xenografts

Mice bearing MDA-MB-231 mammary fad pad tumors were treated with either viral construct. Tumors infected with GLV-1h164 demonstrated a significantly larger tumor volume regression compared to both the negative control ($p<0.05$) and the parent virus (GLV-1h100) ($p<0.05$). By day 36, the average tumor size was 414 mm^3 for the control group and 200 mm^3 for the parent virus group ($p<0.05$). The GLV-1h164-treated mice had

significantly reduced tumor size compared to both groups with a mean volume of 67 mm^3 ($p<0.05$) (Fig. 5).

GLV-1h164-infected tumors exhibit decreased vascular flow compared to parent virus-treated and uninfected control groups

Six mice with tumors of similar size, two from each group, were selected and their tumors were imaged with Doppler ultrasonography. Images showed a noticeably decreased vascular flow in tumors treated with GLV-1h164 compared to tumors infected with GLV-1h100 or uninfected controls (Fig. 6). Images were taken 3 weeks after infection.

GLV-1h164-infected tumors experienced significantly inhibited vasculature *in vivo*

Tissue sections were made from excised tumors in each treatment group and stained with MECA-32 to illustrate endothelial cells. Immunofluorescence revealed the presence of cell nuclei in three groups (blue – stained with DAPI), virus in the two infected treatment groups (green – green fluorescence protein), and decreased vasculature in only GLV-1h164 treatment group (red-MECA-32) (Fig. 7a). The signal intensity of the red fluorescence was quantified and revealed a 2-fold decrease in GLV-1h164-infected samples compared to uninfected controls (Fig. 7b).

DISCUSSION

TNBCs are a subset of breast cancers that lack expression of hormone receptors and the overexpression of the Her2/neu receptor. The lack of these cell surface targets makes this subtype of breast cancer unsusceptible to forms of targeted therapies and creates an unmet need for treatment for these specific tumors. Clinically, TNBCs are characterized by early relapses and metastatic disease, with chemotherapy usually the only therapeutic option for those patients. However, patients with recurrent or metastatic TNBC show a particularly limited duration of response to successive chemotherapy agents [14,15].

Most research studies have focused on key signaling pathways in TNBC to develop new targeted agents. Targeting of the angiogenic factor VEGF has been shown to improve outcomes in human breast cancer patients. The most prominent findings with respect to anti-angiogenic therapy of breast cancer include prolonged progression-free survival in patients with metastatic breast cancer [16–18] treated with bevacizumab, indicating biologic activity of this agent in this disease. These are encouraging results. While the long-term overall survival data remains fully to be elucidated, progression-free survival and recurrence rates are important outcomes metrics for both patients and ongoing research studies to be considered. Moreover, studies of combining multiple therapies have shown improved outcomes with synergistic mechanisms. We therefore hoped to show improved efficacy of a combination drug versus one drug alone in effort to decreasing cytotoxicity and cost.

Our laboratory recently reported promising results using oncolytic vaccinia viral therapy for TNBC [19]. We therefore investigated the therapeutic effect of a novel vaccinia virus expressing an anti-VEGF antibody in an orthotopic murine TNBC model. Our data shows that GLV-1h164 effectively infects and decreases the growth rate of multiple TNBC cell lines *in vitro*. Moreover, we demonstrate unaltered replication efficacy of this novel virus. In

other words, the insertion of the therapeutic gene cassette into the viral genome did not negatively affect or attenuate the previously demonstrated viral replication potential within TNBC. Lastly, we illustrate that GLV-1h164 achieves significant cytotoxicity against orthotopic mammary fat pad tumors *in vivo* by causing decreased vascular density, as demonstrated by our Doppler flow studies and immunostaining of tumor tissues 3 weeks after a single dose or viral therapy in addition to direct oncolysis.

It has been well described that angiogenesis is required for tumor growth and progression. With regards to TNBC, high levels of VEGF have been associated with a less favorable treatment prognosis [12]. For TNBC, there is recent evidence that bevacizumab has therapeutic activity in patients with locally recurrent and metastatic breast cancer [20]. However, the main issue still remains that, like many other targeted therapies, the clinical benefit is modest and is significant only when combined with other therapeutic agents. As these tumors develop resistance to most conventional chemotherapeutic agents relatively quickly [2], we proposed the use of an oncolytic virus for treatment of TNBC. The rationale for this approach is that the mechanisms of oncolytic viral infection and cell lysis are independent of the molecular pathways that drive tumor initiation and growth; thus, treatment with an oncolytic virus should therefore not be affected by conventional pathways of resistance developed in these breast cancer cells. Our recent results show a similar vaccinia virus achieving a significant therapeutic effect in an orthotopic TNBC model. We therefore developed a novel multi-targeted therapeutic agent for TNBC, an oncolytic virus engineered to express an anti-angiogenic antibody in virally-infected cells. This enhancement in therapeutic effect may be caused by the continuous production of the anti-VEGF scAb, which can decrease vascular flow supplying the tumor. Moreover, assessment of microvascular density is becoming more feasible through use of digital micro-imaging and analysis. Increased microvascular density has been associated with higher grade of tumors [21]. As our study demonstrated the efficacy of an anti-angiogenic virus in treatment of TNBC, future work will include examination and measurement of the effects of viral treatment on microvessel density.

Finally, a potential mechanism contributing to the observed enhanced effect of this virus in the current study would potentially be an immunomodulatory effect by the scAb as well as the virus itself. Research has been reported that angiogenic factors including VEGF can decrease the immune response in tumors [22]. In addition, infected breast tumors with VACV have been shown to have an activated innate immune system [23] and potentially cause recruitment of the immune effector cells in the tumor microenvironment [24,25]. Specifically, whether this novel VACV with over-expression of GLAF-2 scAb has an effect on the immune system needs to be further studied.

An additional advantage of oncolytic viruses is that they can serve as vehicles for therapeutic transgenes and thus offer a non-invasive form of therapeutic monitoring. GLV-1h164 has the ability to detect disease to the presence of inserted marker genes (GFP) as illustrated in this study. Fluorescent imaging can assist clinicians by detecting viral distribution in order to monitor therapeutic effects via tumor localization and drug toxicity. Our laboratory has previously shown that this viral reporter gene may be utilized as a predictor of response to therapy [10] and to monitor invasion and metastatic spread in TNBC cells [11]. Lastly, we

note that oncolytic vaccinia therapy is a safe approach as it has been demonstrated to be safely given to millions of patients during the smallpox eradication.

In conclusion, this is the first study to show the therapeutic efficacy of a novel virus, GLV-1h164 carrying an anti-angiogenic scAb (GLAF-2) in vitro and in a xenograft mammary fat pad model. Specifically, we demonstrate significantly enhanced regression of tumor volumes and decreased angiogenesis with ultrasound imaging after a single injection of GLV-1h164 compared to its parent virus in vivo. Altogether, the VACV-mediated delivery and production of a therapeutic anti-VEGF scAb in colonized tumors may offer a tumor-specific, locally amplified drug therapy for patients with TNBC.

Acknowledgments

Technical services provided by the Research Animal Resource Center (RARC), the Molecular Cytology and the Small-Animal Imaging Core Facilities at Memorial Sloan-Kettering Cancer Center are gratefully acknowledged. We also would like to thank Mesruh Turkekul for their excellent technical assistance.

SOURCE OF FINANCIAL SUPPORT: This study was partly supported by a grant from the Mr. William H. and Mrs. Alice Goodwin and the Commonwealth Foundation for Cancer Research and The Experimental Therapeutics Center of Memorial Sloan-Kettering Cancer Center and a grant from the Flight Attendant Medical Research Institute.

References

1. Bauer KR, Brown M, Cress RD, Parise CA, Caggiano V. Descriptive analysis of estrogen receptor (ER)-negative, progesterone receptor (PR)-negative, and HER2-negative invasive breast cancer, the so-called triple-negative phenotype: a population-based study from the California cancer Registry. Cancer. 2007; 109(9):1721–1728. DOI: 10.1002/cncr.22618 [PubMed: 17387718]
2. Dent R, Trudeau M, Pritchard KI, Hanna WM, Kahn HK, Sawka CA, Lickley LA, Rawlinson E, Sun P, Narod SA. Triple-negative breast cancer: clinical features and patterns of recurrence. Clinical cancer research: an official journal of the American Association for Cancer Research. 2007; 13(15 Pt 1):4429–4434. DOI: 10.1158/1078-0432.CCR-06-3045 [PubMed: 17671126]
3. Ismail-Khan R, Bui MM. A review of triple-negative breast cancer. Cancer control: journal of the Moffitt Cancer Center. 2010; 17(3):173–176. [PubMed: 20664514]
4. Linderholm BK, Hellborg H, Johansson U, Elmberger G, Skoog L, Lehtio J, Lewensohn R. Significantly higher levels of vascular endothelial growth factor (VEGF) and shorter survival times for patients with primary operable triple-negative breast cancer. Annals of oncology: official journal of the European Society for Medical Oncology/ESMO. 2009; 20(10):1639–1646. DOI: 10.1093/annonc/mdp062
5. Khosravi Shahi P, Soria Lovelle A, Perez Manga G. Tumoral angiogenesis and breast cancer. Clinical & translational oncology: official publication of the Federation of Spanish Oncology Societies and of the National Cancer Institute of Mexico. 2009; 11(3):138–142.
6. Wang N, Wang ZY, Mo SL, Loo TY, Wang DM, Luo HB, Yang DP, Chen YL, Shen JG, Chen JP. Ellagic acid, a phenolic compound, exerts anti-angiogenesis effects via VEGFR-2 signaling pathway in breast cancer. Breast cancer research and treatment. 2012; 134(3):943–955. DOI: 10.1007/s10549-012-1977-9 [PubMed: 22350787]
7. Gholami S, Haddad D, Chen CH, Chen NG, Zhang Q, Zanzonico PB, Szalay AA, Fong Y. Novel therapy for anaplastic thyroid carcinoma cells using an oncolytic vaccinia virus carrying the human sodium iodide symporter. Surgery. 2011; 150(6):1040–1047. DOI: 10.1016/j.surg.2011.09.010 [PubMed: 22136819]
8. Haddad D, Chen NG, Zhang Q, Chen CH, Yu YA, Gonzalez L, Carpenter SG, Carson J, Au J, Mittra A, Gonen M, Zanzonico PB, Fong Y, Szalay AA. Insertion of the human sodium iodide symporter to facilitate deep tissue imaging does not alter oncolytic or replication capability of a novel vaccinia

virus. Journal of translational medicine. 2011; 9:36.doi: 10.1186/1479-5876-9-36 [PubMed: 21453532]

9. Lun XQ, Jang JH, Tang N, Deng H, Head R, Bell JC, Stojdl DF, Nutt CL, Senger DL, Forsyth PA, McCart JA. Efficacy of systemically administered oncolytic vaccinia virotherapy for malignant gliomas is enhanced by combination therapy with rapamycin or cyclophosphamide. Clinical cancer research: an official journal of the American Association for Cancer Research. 2009; 15(8):2777–2788. DOI: 10.1158/1078-0432.CCR-08-2342 [PubMed: 19351762]
10. Haddad D, Chen N, Zhang Q, Chen CH, Yu YA, Gonzalez L, Aguilar J, Li P, Wong J, Szalay AA, Fong Y. A novel genetically modified oncolytic vaccinia virus in experimental models is effective against a wide range of human cancers. Annals of surgical oncology. 2012; 19(Suppl 3):S665–674. DOI: 10.1245/s10434-011-2198-x [PubMed: 22258815]
11. Gholami S, Chen CH, Belin LJ, Lou E, Fujisawa S, Antonacci C, Carew A, Chen NG, De Brot M, Zanzonico PB, Szalay AA, Fong Y. Vaccinia virus GLV-1h153 is a novel agent for detection and effective local control of positive surgical margins for breast cancer. Breast cancer research: BCR. 2013; 15(2):R26.doi: 10.1186/bcr3404 [PubMed: 23506710]
12. Frentzen A, Yu YA, Chen N, Zhang Q, Weibel S, Raab V, Szalay AA. Anti-VEGF single-chain antibody GLAF-1 encoded by oncolytic vaccinia virus significantly enhances antitumor therapy. Proceedings of the National Academy of Sciences of the United States of America. 2009; 106(31):12915–12920. DOI: 10.1073/pnas.0900660106 [PubMed: 19617539]
13. Chen N, Zhang Q, Yu YA, Stritzker J, Brader P, Schirbel A, Samnick S, Serganova I, Blasberg R, Fong Y, Szalay AA. A novel recombinant vaccinia virus expressing the human norepinephrine transporter retains oncolytic potential and facilitates deep-tissue imaging. Molecular medicine. 2009; 15(5–6):144–151. DOI: 10.2119/molmed.2009.00014 [PubMed: 19287510]
14. Lin NU, Claus E, Sohl J, Razzak AR, Arnaout A, Winer EP. Sites of distant recurrence and clinical outcomes in patients with metastatic triple-negative breast cancer: high incidence of central nervous system metastases. Cancer. 2008; 113(10):2638–2645. DOI: 10.1002/cncr.23930 [PubMed: 18833576]
15. Kassam F, Enright K, Dent R, Dranitsaris G, Myers J, Flynn C, Fralick M, Kumar R, Clemons M. Survival outcomes for patients with metastatic triple-negative breast cancer: implications for clinical practice and trial design. Clinical breast cancer. 2009; 9(1):29–33. DOI: 10.3816/CBC.2009.n.005 [PubMed: 19299237]
16. Mackey JR, Kerbel RS, Gelmon KA, McLeod DM, Chia SK, Rayson D, Verma S, Collins LL, Paterson AH, Robidoux A, Pritchard KI. Controlling angiogenesis in breast cancer: a systematic review of anti-angiogenic trials. Cancer treatment reviews. 2012; 38(6):673–688. DOI: 10.1016/j.ctrv.2011.12.002 [PubMed: 22365657]
17. Miller K, Wang M, Gralow J, Dickler M, Cobleigh M, Perez EA, Shenkier T, Cella D, Davidson NE. Paclitaxel plus bevacizumab versus paclitaxel alone for metastatic breast cancer. The New England journal of medicine. 2007; 357(26):2666–2676. DOI: 10.1056/NEJMoa072113 [PubMed: 18160686]
18. Robert NJ, Dieras V, Glaspy J, Brufsky AM, Bondarenko I, Lipatov ON, Perez EA, Yardley DA, Chan SY, Zhou X, Phan SC, O'Shaughnessy J. RIBBON-1: randomized, double-blind, placebo-controlled, phase III trial of chemotherapy with or without bevacizumab for first-line treatment of human epidermal growth factor receptor 2-negative, locally recurrent or metastatic breast cancer. Journal of clinical oncology: official journal of the American Society of Clinical Oncology. 2011; 29(10):1252–1260. DOI: 10.1200/JCO.2010.28.0982 [PubMed: 21383283]
19. Gholami S, Chen CH, Lou E, De Brot M, Fujisawa S, Chen NG, Szalay AA, Fong Y. Vaccinia virus GLV-1h153 is effective in treating and preventing metastatic triple-negative breast cancer. Annals of surgery. 2012; 256(3):437–445. DOI: 10.1097/SLA.0b013e3182654572 [PubMed: 22868370]
20. Kerbel RS. Strategies for improving the clinical benefit of antiangiogenic drug based therapies for breast cancer. Journal of mammary gland biology and neoplasia. 2012; 17(3–4):229–239. DOI: 10.1007/s10911-012-9266-0 [PubMed: 23011602]
21. Barau A, Ruiz-Sauri A, Valencia G, Gomez-Mateo Mdel C, Sabater L, Ferrandez A, Llombart-Bosch A. High microvessel density in pancreatic ductal adenocarcinoma is associated with high

grade. Virchows Archiv: an international journal of pathology. 2013; 462(5):541–546. DOI: 10.1007/s00428-013-1409-1 [PubMed: 23579431]

22. Gabrilovich DI, Ishida T, Nadaf S, Ohm JE, Carbone DP. Antibodies to vascular endothelial growth factor enhance the efficacy of cancer immunotherapy by improving endogenous dendritic cell function. Clinical cancer research: an official journal of the American Association for Cancer Research. 1999; 5(10):2963–2970. [PubMed: 10537366]
23. Zhang Q, Yu YA, Wang E, Chen N, Danner RL, Munson PJ, Marincola FM, Szalay AA. Eradication of solid human breast tumors in nude mice with an intravenously injected light-emitting oncolytic vaccinia virus. Cancer research. 2007; 67(20):10038–10046. DOI: 10.1158/0008-5472.CAN-07-0146 [PubMed: 17942938]
24. Mantovani A, Romero P, Palucka AK, Marincola FM. Tumour immunity: effector response to tumour and role of the microenvironment. Lancet. 2008; 371(9614):771–783. DOI: 10.1016/S0140-6736(08)60241-X [PubMed: 18275997]
25. Thorne SH, Bartlett DL, Kirn DH. The use of oncolytic vaccinia viruses in the treatment of cancer: a new role for an old ally? Current gene therapy. 2005; 5(4):429–443. [PubMed: 16101516]

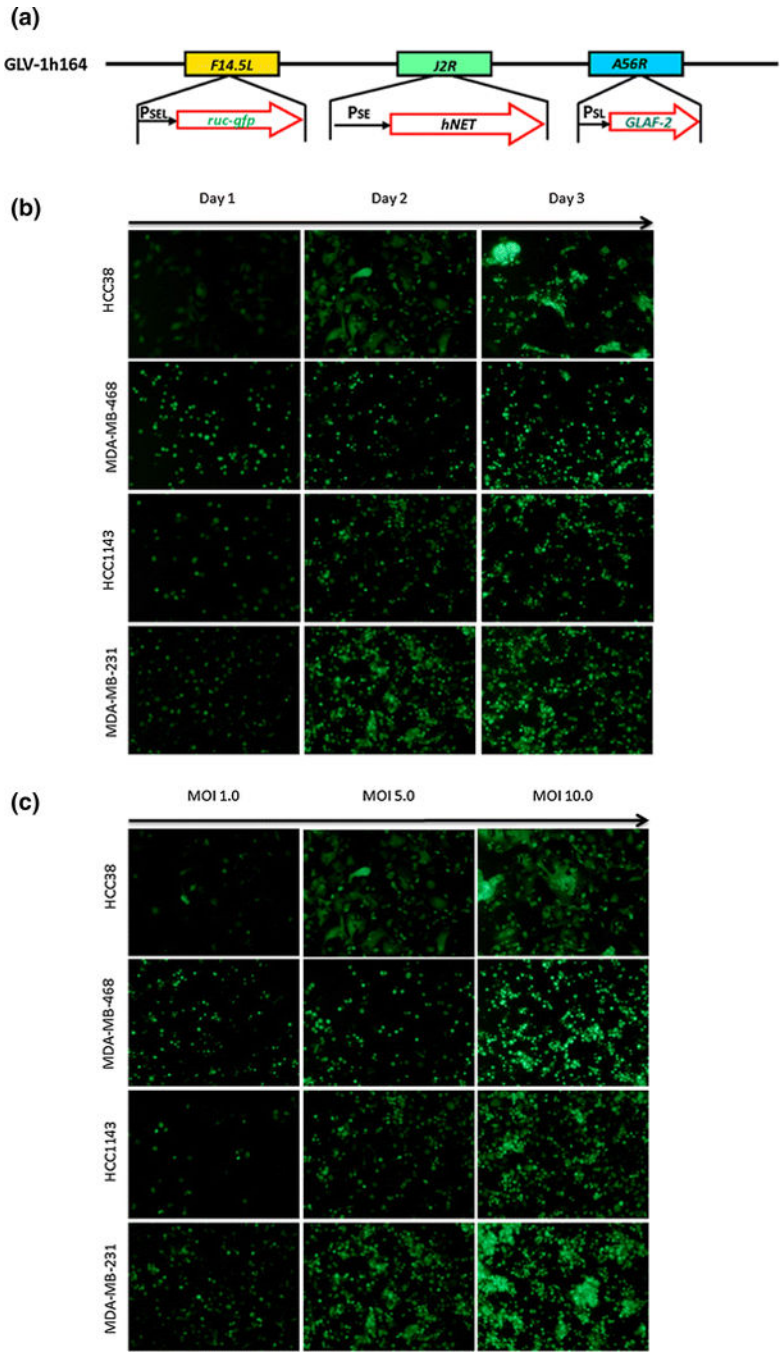

Figure 1.

(a) Viral constructs of GLV-1h164 and Glv1h100. (b) *In vitro* viral infection of TNBC cell lines at MOI 5 across 3 days. GFP expression in infected cells is shown by green fluorescence. Vertical axis demonstrates TNBC cells lines and horizontal axis shows days after infection. All cells were infected at an MOI of 5. **(c) *In vitro* viral infection of TNBC cell lines on day 2 with varying viral dosages.**

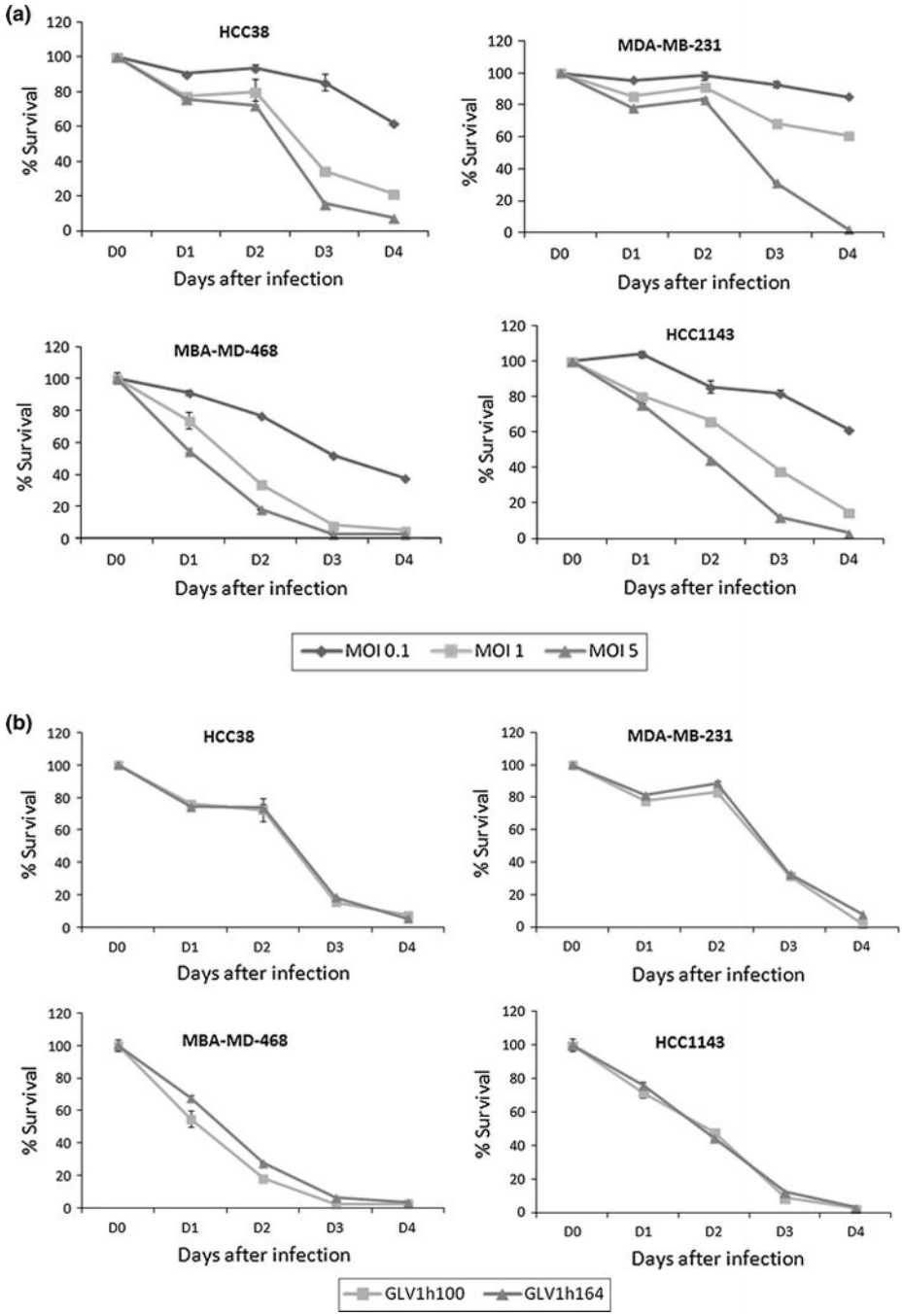

Figure 2.

(a) Percent survival of TNBC cells after GLV-1h164 infection *in vitro*. Mean % of cell survival was measured at 3 MOIs over the course of 4 days. (MOI = Multiplicity of infection, # plaque-forming units/cell). **(b) Percent survival of TNBC cells after infection with GLV-1h164 vs. GLV-1h100 (parent virus) *in vitro*.** Mean % of cell survival was measured at MOI 5 over the course of 5 days in all TNBC cell lines.

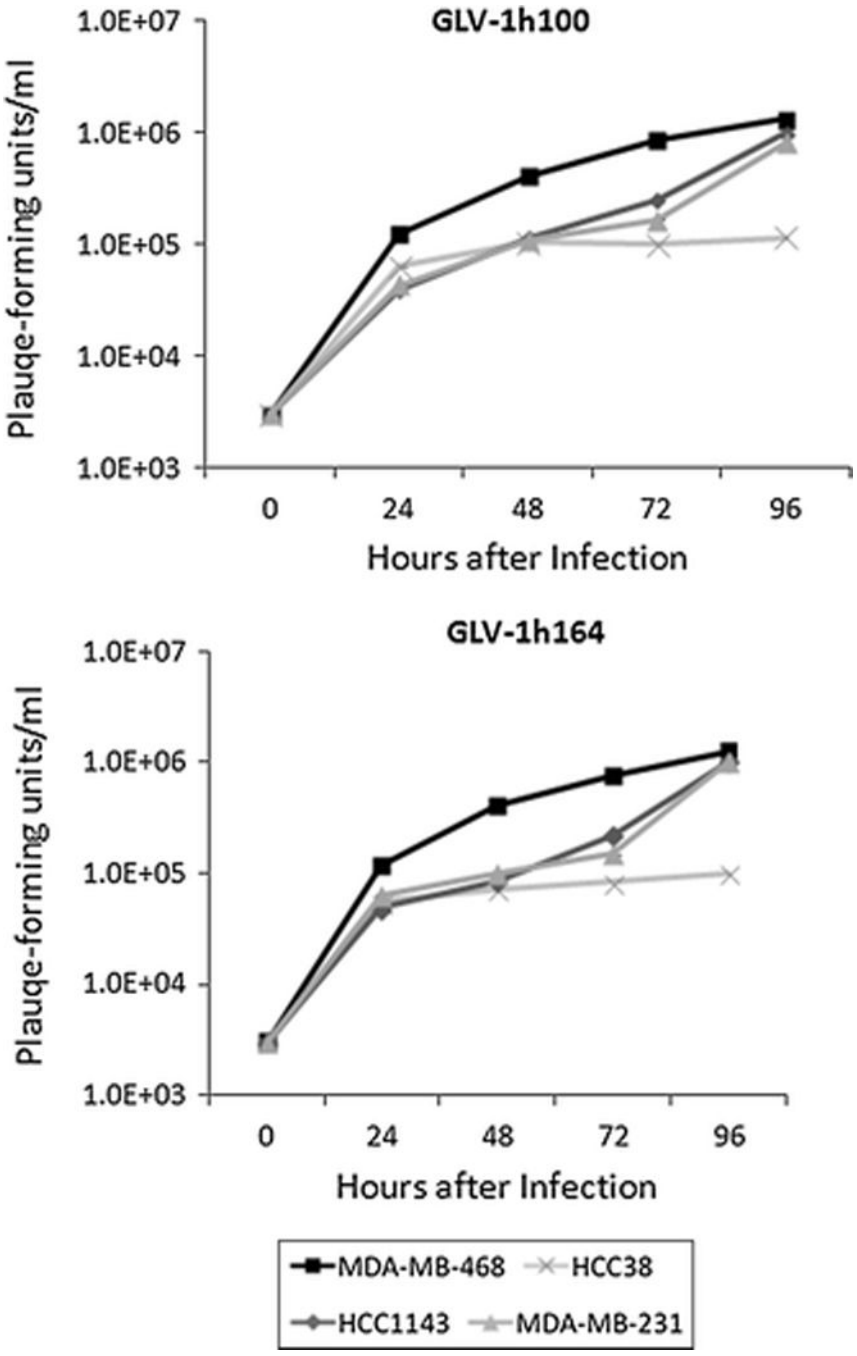

Figure 3. Replication efficiency of GLV-1h164 vs. GLV-1h100 in TNBC cells *in vitro*

Standard viral plaque assays were performed daily and number of viral plaque-forming units were counted and are represented on the y-axis.

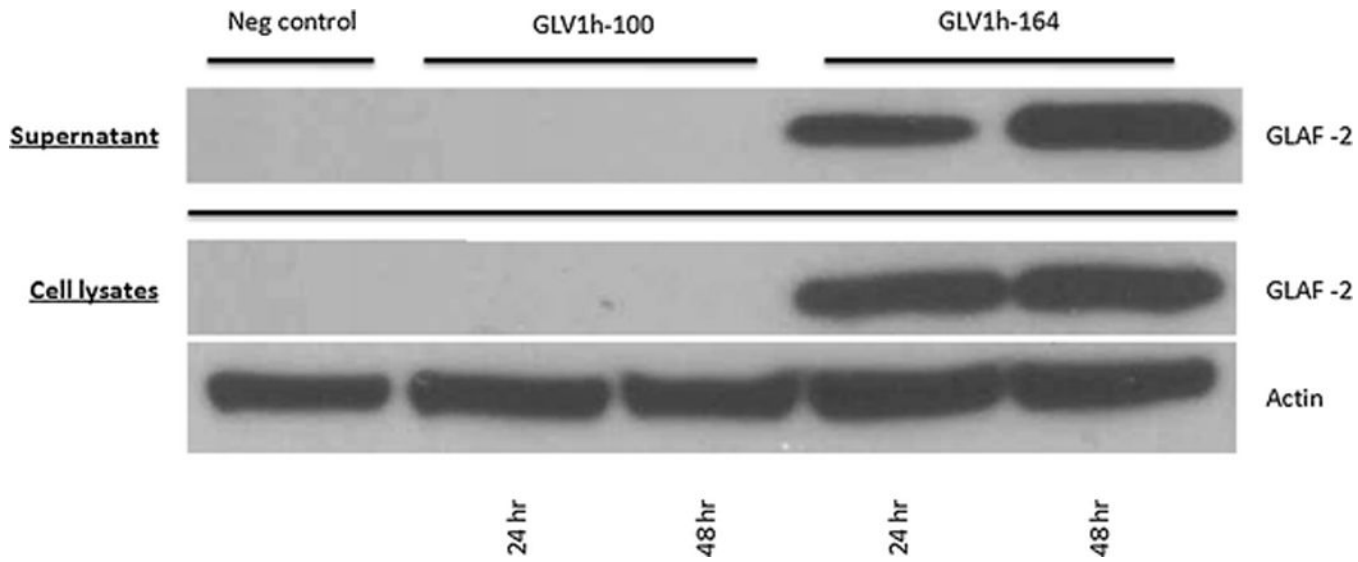

Figure 4. Expression of anti-VEGF antibody GLAF-2 in tumor cell lysates and culture supernatants of GLV-1h164-infected cells, as demonstrated by Western blotting

MDA-MB-468 cells were infected with either vaccinia strain at an MOI of 1.0 or media (for controls) for up to 48 hours. Western blotting was performed with an anti-GLAF-2 antibody.

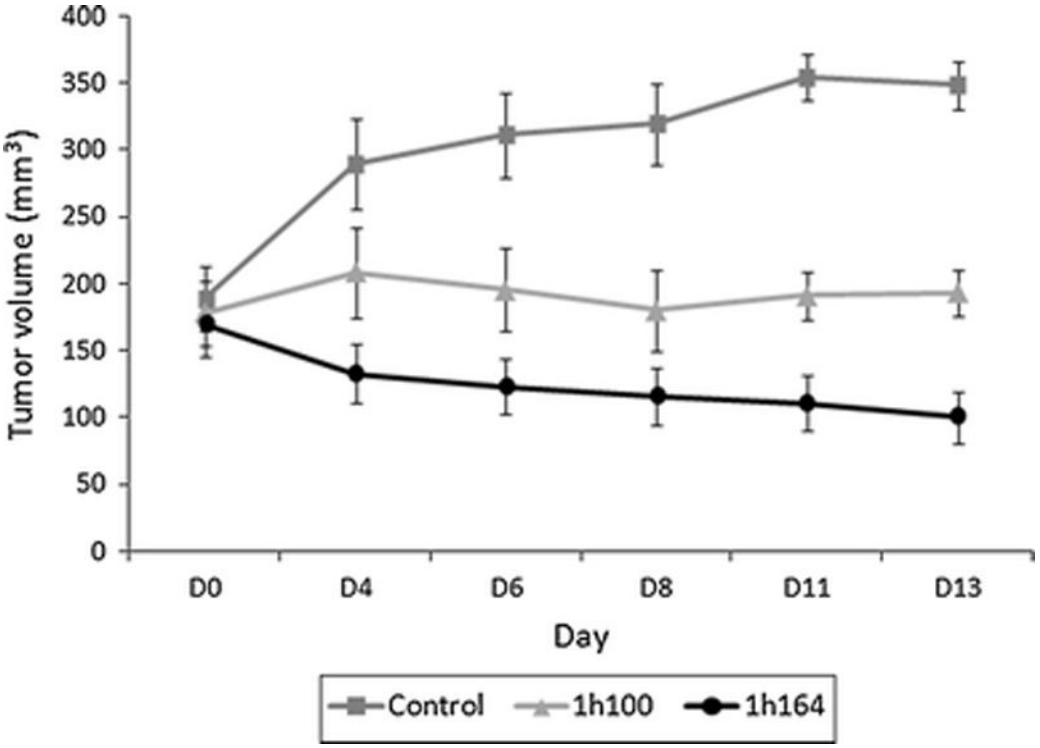

Figure 5. Tumor volume of mammary fat pad xenografts in untreated, GLV-1h100, and GLV-1h164 treatment groups *in vivo*

Tumors were injected with either virus or PBS (control) 2 weeks after tumor formation (D0). Tumor volumes were measured three times a week.

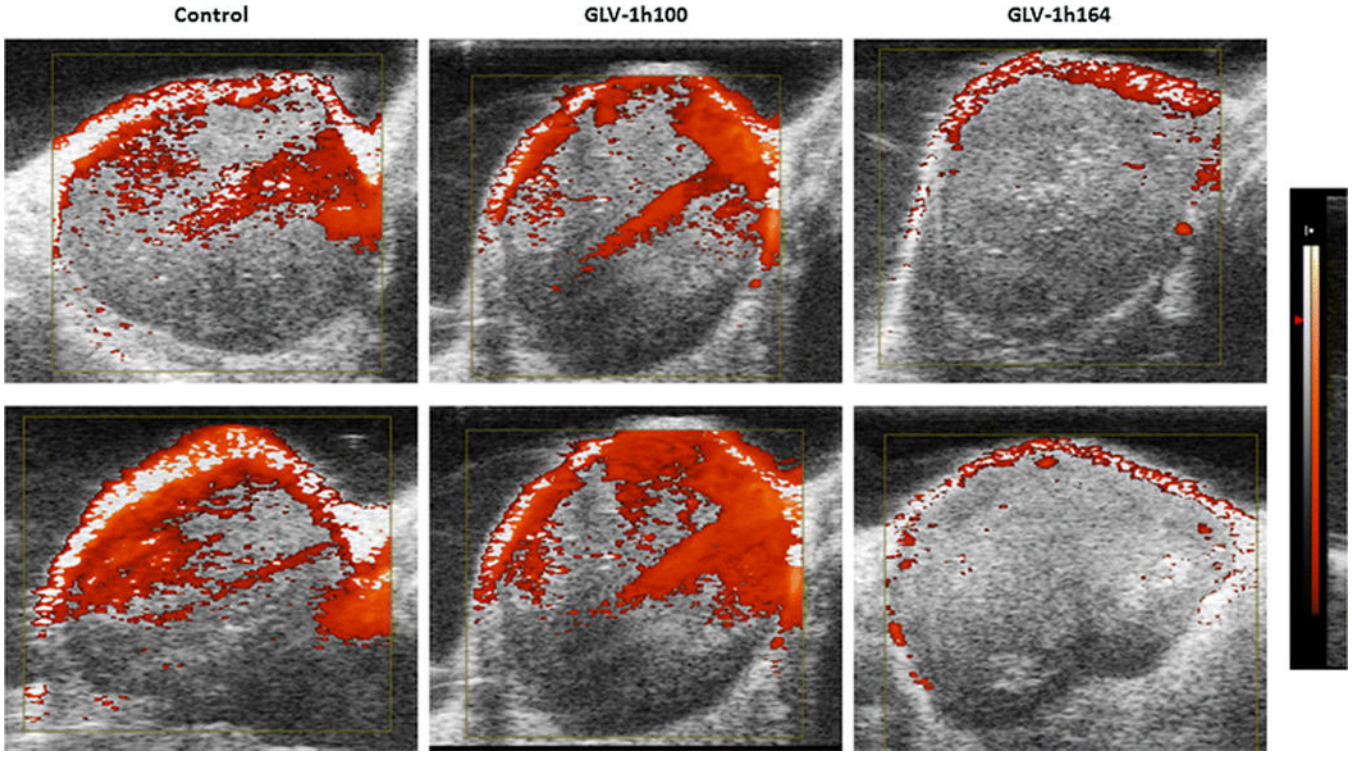

Figure 6. Doppler ultrasonography measurement of vascular flow in controls, GLV-1h100-, and GLV-1h164-infected tumors *in vivo*

Two tumors from each treatment group were separately treated for 3 weeks and imaged with Doppler ultrasonography. The Doppler-derived relative tissue perfusion image was displayed in a “hot-iron” color scale superimposed on a gray-scale B-mode image, with lack of the hot-iron coloration corresponding to lower perfusion. Equal-size tumors were selected to avoid tumor size as confounding factor for vascular flow.

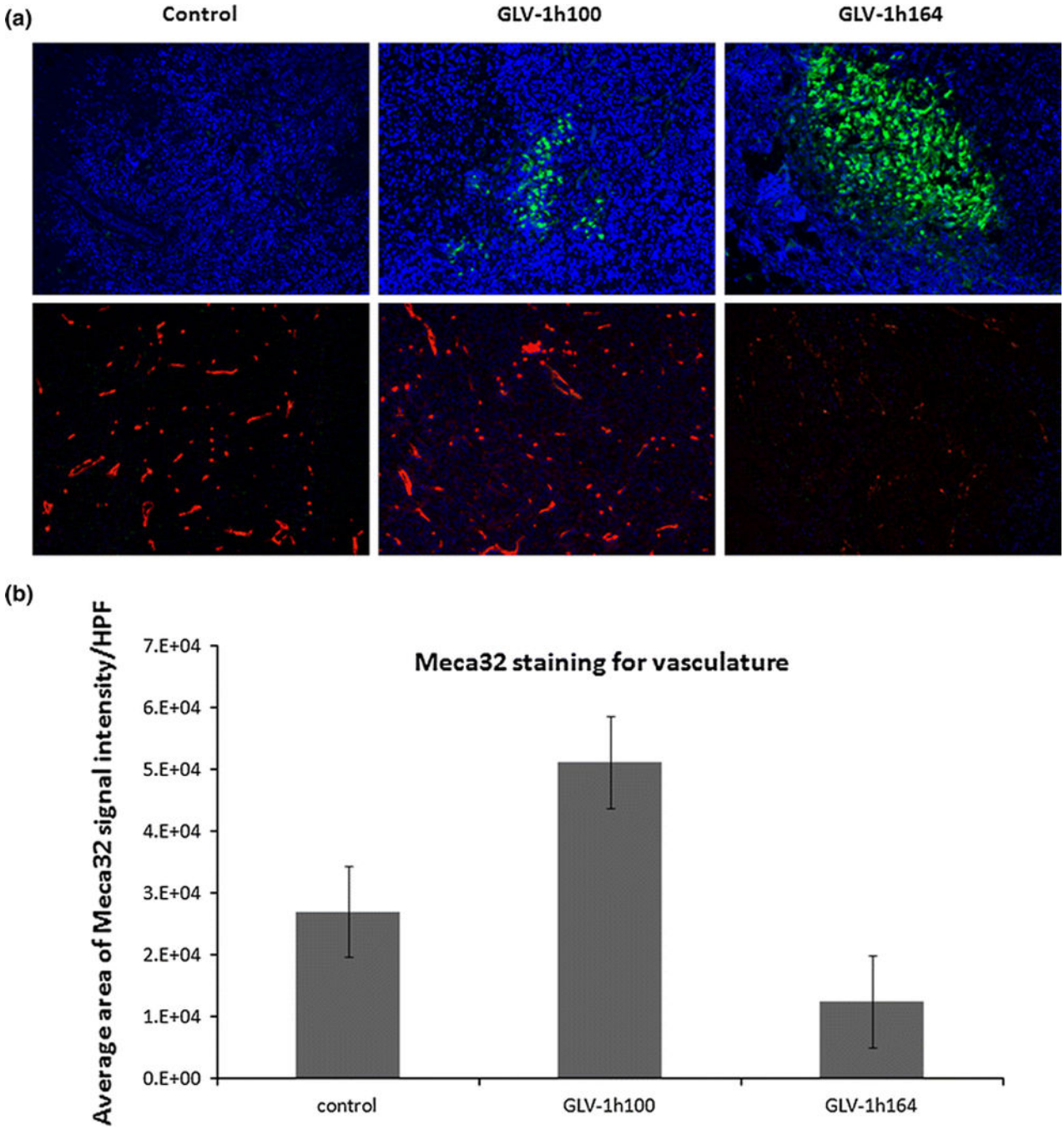

Figure 7.

(a) Immunofluorescence of endothelial cells in each treatment group *in vivo*. Only viral-infected groups show expression of green fluorescent protein (GFP). Endothelial cells of excised tumors from each treatment group were stained with MECA-32 (red). Cell nuclei are expressed with DAPI (blue). **(b) Quantification of endothelial cell signal intensity for controls and GLV-1h164 treatment group *in vivo*.** Measured areas of signal intensity/HPF

were obtained from averaging a total of 15 images from 3 individual sections per treatment group.